



Chemical inhibition of LSD1 leads to epithelial to mesenchymal transition *in vitro* of an oral squamous cell carcinoma OM-1 cell line *via* release from LSD1-dependent suppression of *ZEB1*



Nao Yamakado, Satoshi Okuda, Kei Tobiume*, Ryo Uetsuki, Shigehiro Ono, Kuniko Mizuta, Takayuki Nakagawa, Tomonao Aikawa

Department of Oral and Maxillofacial Surgery, Graduate School of Biomedical & Health Sciences, Hiroshima University, Hiroshima, Japan

ARTICLE INFO

Article history:

Received 23 December 2022

Received in revised form

4 January 2023

Accepted 19 January 2023

Available online 25 January 2023

ABSTRACT

The epigenetic regulation for gene expression determines cell plasticity. Oral squamous cell carcinoma (SCC) exhibits bidirectional cell plasticity, *i.e.* epithelial differentiation and epithelial to mesenchymal transition (EMT). The epigenetic regulator LSD1 is a histone H3-specific demethylase to which chemical inhibitors for its activity had been developed as an anti-cancer therapeutics. The bidirectional plasticity of the oral SCC cell line OM-1 had been characterized, but it remained unclear how chemical LSD1 inhibitors affect cell plasticity. Here we reported an adverse effect against cancer therapeutics, which was EMT induction *in vitro* by the chemical LSD1 inhibitor. The LSD1 inhibitor caused EMT-TF *ZEB1* in OM-1 to undergo EMT. Furthermore, an additional EMT-TF Snail-dependent partial EMT phenotype in OM-1 progressed to complete EMT in conjunction with LSD1 inhibitor-dependent *ZEB1* induction. The promoter activity of *ZEB1* was up-regulated under LSD1 inhibition. The regulatory chromatin regions of *ZEB1* accumulated histone H3 methylation under the chemical inhibition of LSD1. The LSD1 inhibitor also upregulates epithelial gene expression *in vitro*; however, the bidirectional effect of LSD1 inhibitor should be considered in cancer therapeutics.

© 2023 Elsevier Inc. All rights reserved.

1. Introduction

EMT is regulated by transcription factors (TFs), including the Snail family, *ZEB1* family, and Twist family, referred to as EMT-TFs. The EMT-TF functions to cause the loss of epithelial hemophilic adhesion and conversion of the cytoskeleton to mesenchymal Vimentin, leading to invasive progression of the malignant epithelial tumor [1]. Histone lysine-specific demethylase1 (LSD1) plays a crucial part in the physiological process of cell fate determination [2,3]. Targeting LSD1 is recognized as a promising therapeutic option for malignant tumor treatment [4,5]. It has been demonstrated that inhibiting LSD1 promotes epithelial differentiation in cancer cells; therefore, LSD1 inhibitors are highly anticipated as a cancer treatment drug [6].

Snail family EMT-TFs associate with LSD1 via the SNUG motif to

silence *Snail*-target genes through histone demethylation [7]. Therefore, it was believed that LSD1 was linked to cancer malignancy via EMT [8,9].

The present study, aimed to unveil the efficacy of LSD1 inhibitors on OM-1 cells with opposing cell-fate in cell culture, namely epithelial differentiation and mesenchymal transition. The findings showed that the LSD1 inhibitor induce EMT through the release of LSD1-dependent histone demethylation at an EMT-TF *ZEB1* regulating chromatin region.

2. Materials and methods

2.1. Cell culture

The human oral SCC cell line OM-1 and its subclone pEMT OM-1^{Snail} have been previously described [10]. HEK293 was purchased from the RIKEN cell bank, Tsukuba, Japan. The cells were cultured at 37 °C in a humidified atmosphere of 5% CO₂ in the air and maintained in DMEM (#D6429, Sigma-Aldrich, St. Louis, MO, USA) supplemented with 10% fetal bovine serum (Sigma-Aldrich).

* Corresponding author. Graduate School of Biomedical and Health Sciences, Hiroshima University, 1-2-3 Kasumi, Minami-ku, Hiroshima, 734-8553, Japan.

E-mail address: tobi5651@hiroshima-u.ac.jp (K. Tobiume).

2.2. Reverse transcription polymerase chain reaction (RT-PCR)

Total RNA was isolated using an RNeasy Mini Kit for the RT-PCR analysis (Qiagen, Hilden, Germany). First-strand cDNA libraries were synthesized using ReverTra Ace qPCR RT Kit (Toyobo, Osaka, Japan). RT-PCR was performed using Go Taq Green Master Mix (Promega, Madison, WI, USA) for 30 cycles of denaturation at 95 °C for 30 s, annealing at 60 °C for 30 s, and extension at 72 °C for 40 s. The PCR products were analyzed using 2% agarose gel electrophoresis. Real-time PCR was performed using Thunderbird SYBR qPCR Mix (Toyobo, Osaka, Japan) and analyzed using Thermal Cycler Dice Real-Time System III (TAKARA BIO, Shiga, Japan). The collected data were evaluated by the $\Delta\Delta C_t$ method with GAPDH as an internal control. The following are the PCR primers and amplicon sizes.

- CDH1 (131 bp): 5'-GCCTCTGAAAAGAGAGTGGAAAG-3' and 5'-TGGCAGTGTCTCTCCAAATCCG-3'
- Vimentin (750 bp): 5'-TGGCAGCTCTTGACCTTGA-3' and 5'-GGTCATCGTGATGCTGAGAA-3'
- Snai1 (321 bp): 5'-AATCGGAAGCCTAACTACAG-3' and 5'-GGAA-GAGACTGAAGTAGAG-3'
- ZEB1 (155 bp): 5'-GGCATACTACTCAACTACGG-3' and 5'-TGGGCGGTGTAGAATCAGAGTC-3'
- OVOL2 (141 bp): 5'-CCACAACCAGGTGAAAAGACACC-3' and 5'-CGCTGGTGAAGCCTTATTGC-3'
- GRHL1 (182 bp): 5'-AACCGCAGCAACAAGCCTGTGC-3' and 5'-TGAGAGGGAAGCAGTGGCACTT-3'
- GRHL2 (155 bp): 5'-CGCTATCTCAAAGACACCAG-3' and 5'-CCAGGTTACTGAAATGTGCC-3'

- GRHL3 (103 bp): 5'-G ACTGTGGAGCACATTGAGGAGG-3' and 5'-CTGTGCTCAGACAGTTTACGCC-3'
- GAPDH (373 bp): 5'-ACCACAGTCCATGCCATCAC-3' and 5'-CAGCCCCAGCGTCAAAGGTG-3'

2.3. Reagents and antibodies

200 M Tranylcpromine (TCP) (Selleck Chemicals, TX, USA) was applied in culture unless otherwise specified. 2 μ M GSK-LSD1 2HCl (Selleck Chemicals) was applied to the culture medium unless otherwise noted. The antibodies and dilution ratios used in immunocytochemistry were as follows: anti-E-cadherin rabbit monoclonal antibody (clone 24E10, 1:200, #3195, Cell Signaling Technology, Danvers, MA, USA), anti-Vimentin mouse monoclonal antibody (clone RV202, 1:200, sc-32322, Santa Cruz Technology, Dallas, TX, USA), and anti-ZEB1 Rabbit monoclonal antibody (clone D80D3, 1:200, #3396, Cell Signaling Technology). The validated antibodies and dilution ratios used in ChIP were as follows: anti-KDM1/LSD1 rabbit monoclonal antibody (clone EPR6825, 1:40, ab129195, abcam, Cambridge, UK) and anti-Histone H3K4me2 mouse monoclonal antibody (clone MABI0303, 1:40, No: 39679, Active Motif, Carlsbad, CA, USA).

2.4. Wound healing assay

OM-1 cells were seeded into six well plates. The cells were allowed to grow to reach 100% confluency. Followed by the addition of TCP to the culture medium for 12 h and 24 h prior to making a

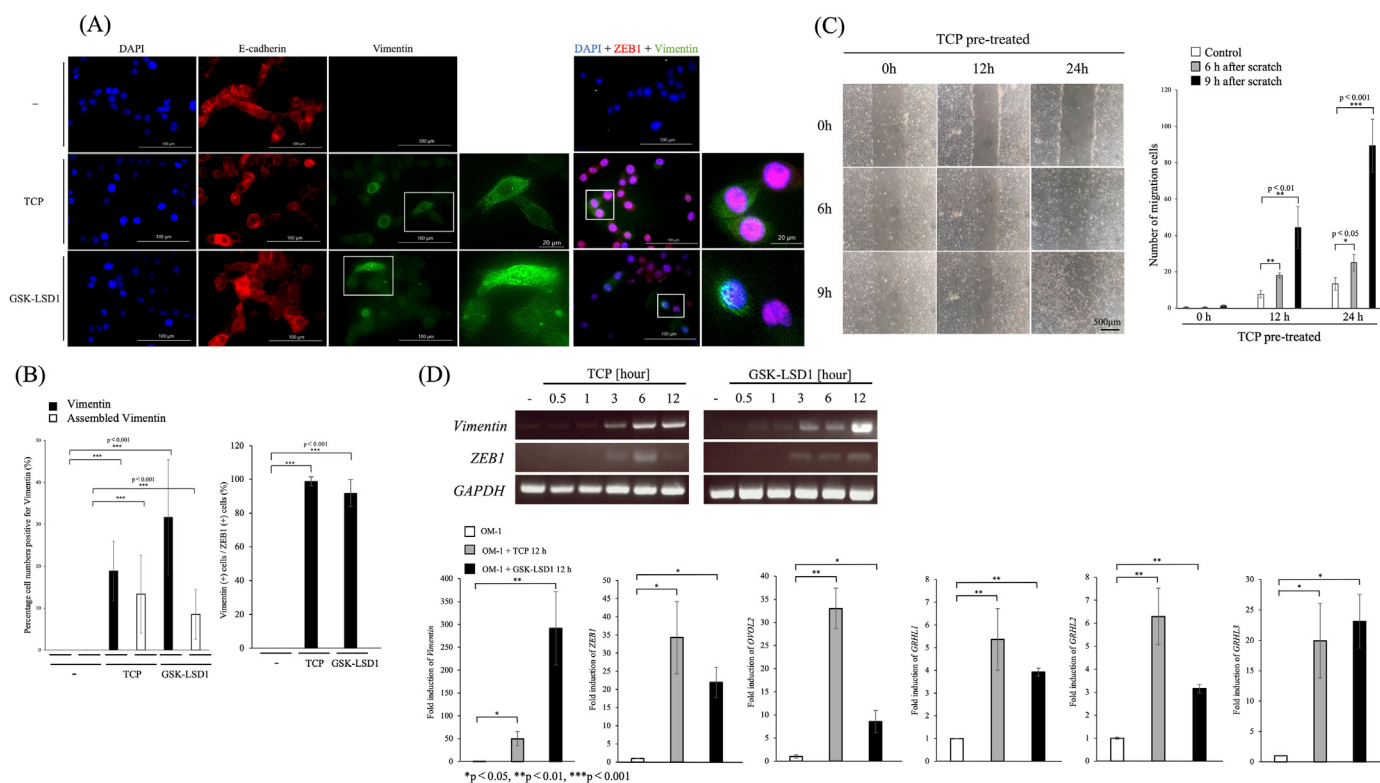


Fig. 1. LSD1 inhibitor-induced ZEB1 and Vimentin in epithelial phenotype OM-1 (A) Immunocytochemistry of OM-1 cell. TCP (200 μ M) and GSK-LSD1 (2 μ M) were added for 12 h. The cells were double stained as indicated. Nuclei were stained with DAPI. Inset areas (white square) were also displayed at higher magnification to show the representative assembled Vimentin image. (B) Percentage cell numbers positive for Vimentin, assembled Vimentin, and ZEB1. Results were from 3 experiments with SD. Statistical analyses were performed between indicated groups. (C) Wound healing assay of OM-1 cell with TCP pre-treated as indicated on top before wounding. Images were taken 0, 6, and 9 h after wounding (top, middle, and bottom panels, respectively). A number of migration cells. Counts were taken from 5 experiments with SD. Statistical analyses were performed between indicated groups. (D) The Vimentin and ZEB1 expression profiles of OM-1 cells treated with LSD1 inhibitors as indicated. The quantified mRNA expression changes of indicated gene upon 12 h of LSD1 inhibitor treatment. Results were from 3 experiments with SD. Statistical analysis were performed between indicated groups.

scratch. The plate was scratched using a 200 μ l pipette tip. Subsequently, images were collected using a BZ-X810 fluorescence microscope (KEYENCE, Osaka, Japan).

2.5. RNA interference

siRNAs targeting *ZEB1* (HSS110548, HSS110549, HSS186235) were purchased from Invitrogen, Carlsbad, CA, USA. Following the manufacturer's instructions, transfection was performed using lipofectamine RNAiMAX (Invitrogen).

2.6. Chromatin immunoprecipitation (ChIP)

ChIP was performed using ChIP-IT[®] Express (Active Motif, #53008) according to the manufacturer's instructions. Briefly, OM-1 and pEMT OM-1^{Snai1} cells were fixed for 10 min by adding 37% formaldehyde. Next, nuclei isolation was performed by Dounce Homogenizer (Active motif, #40401). Shearing of chromatin was performed by Bioruptor UCD-250 (Cosmo Bio, Tokyo, Japan) for 20 pulses of 30 s each, followed by 30 s of rest on ice. The target chromatin regions were detected using Thunderbird SYBR qPCR Mix (Toyobo) and Thermal Cycler Dice Real-Time System III (TAKARA BIO). The percentage of immunoprecipitated chromatin relative to the amount of starting chromatin was determined. The outcome was expressed as a fold change between LSD1 inhibition and the control. The target primers are listed below.

1 (163 bp): 5'-ACGTTCTACGCGAGGAAGA-3' and 5'-GCTA-GAAGTCCGCTTGCCA-3'

2 (103 bp): 5'-CAGGTAGCCTCTCCGGT-3' and 5'-GGAAAGGGATCGCGGTCTG-3'

3 (184 bp): 5'-CGTGGACTGATGGTAGCC-3' and 5'-AAGG-TAAAGTTGAGGCTCGG-3'

4 (117 bp): 5'-TTCTGACCGCGTCCCTACG-3' and 5'-GTTTGCGCAACCGTGG-3'

5 (115 bp): 5'-AAAGTGGAGTGGGAAAGTAGAAAGT-3' and 5'-GACCAGTAAGAGACATAACGGT-3'

6 (111 bp): 5'-GATTTGTCTGCTGTGCCAA-3' and 5'-GCAAC-CACCACCACATGTTC-3'

7 (175 bp): 5'-GCCCCGTACTGTTTGTAT-3' and 5'-CGCGTCCCATTATAGACGCA-3'

8 (144 bp): 5'-TGCGTCTATAATGGGACCGC-3' and 5'-AAAACCTCGGTTTCGCATC-3'

2.7. Immunocytochemistry

Cells were cultured in chamber slide plates (Nunc Lab-Tek II Chamber Slide System, Thermo Fisher Scientific, Waltham, MA, USA). The cells were fixed with 4% paraformaldehyde in phosphate-buffered saline (PBS) for 30 min. Following blocking and permeabilization with 0.3% Triton X-100, 5% BSA in PBS (all from Sigma-Aldrich) for 1 h, the cells were incubated with antibodies in 0.3% Triton X-100, 5% BSA in PBS for 12 h at 4 °C. Antibody binding was visualized with Alexa Fluor 568 goat anti-rabbit IgG (H + L) (A-11036, Invitrogen) or Alexa Fluor 488 goat anti-mouse IgG (A-11001, Invitrogen), diluted 1:10,000 in PBS for 1 h. Images were analyzed using a BZ-X810 fluorescence microscope following

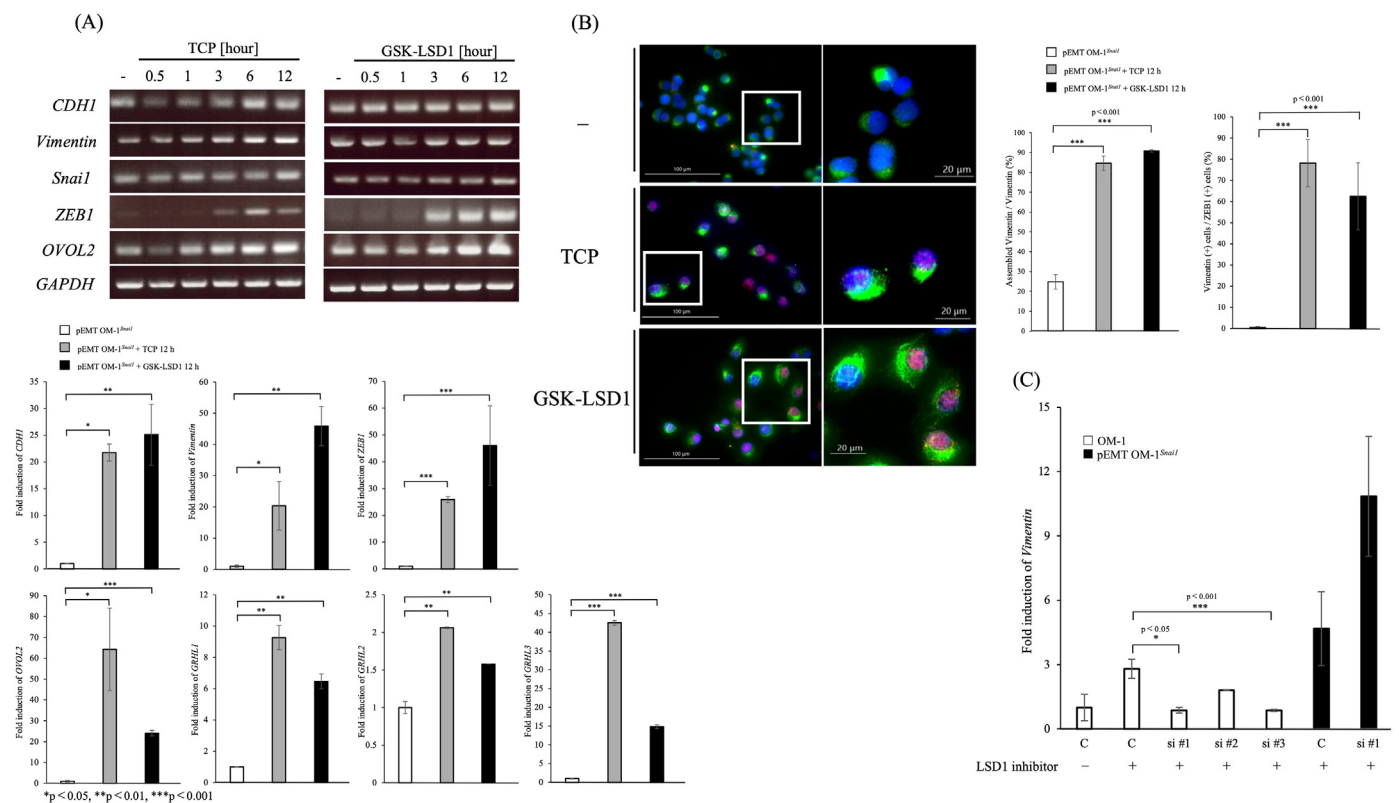


Fig. 2. LSD1 inhibitor-induced *ZEB1* and promoted EMT in partial EMT phenotype OM-1. (A) The representative mRNA expression profiles of pEMT OM-1^{Snai1} cells in response to LSD1 inhibitors. The quantified mRNA expression changes of indicated gene upon 12 h of LSD1 inhibitor treatment. Results were from 3 experiments with SD. Statistical analysis were performed between indicated groups. (B) Immunocytochemistry of pEMT OM-1^{Snai1} cells with or without LSD1 inhibitor treatment for 12 h. All panels were double stained with anti-Vimentin and anti-ZEB1 antibodies. Nuclei were stained with DAPI. The insets in images (white square) were displayed in higher magnification to demonstrate the assembled Vimentin. Percentage cell numbers with the assembled Vimentin (left diagram) and with ZEB1 (right diagram) were determined from 3 experiments with SD. Statistical analyses were performed between indicated groups. (C) Quantified Vimentin expression changes by *ZEB1* knockdown in OM-1 cells and pEMT OM-1^{Snai1} cells. The validation for silencing effects by each siZEB1 were displayed in the supplemental figure.

mounting with 4',6-diamidino-2-phenylindole (DAPI) containing VECTASHIELD (Vector Laboratories Inc., Burlingame, CA, USA) (KEYENCE).

2.8. Luciferase reporter assay

Transcription start sites (TSSs) of *ZEB1* were identified using the Eukaryotic Promoter Database (<https://epd.epfl.ch>) followed by cloning of -3000 to 100 sequences of *ZEB1_4* into pUC57. The sequence contained two alternative promoters which could be separated by XhoI digestion. SacI-XhoI or XhoI-HindIII fragments from pUC57 were cloned into pGL4.10 (Promega) to generate 5' promoter and 3' promoter reporter plasmids, respectively. 70% confluence HEK293 cells were seeded in 12-well plates. The reporter plasmid (1 µg) and pRL-SV40 0.1 µg (Promega) were co-transfected using FuGENE HD Transfection Reagent (Promega) according to the manufacturer's instructions.

Luciferase activities were determined using the Dual-Luciferase reporter assay system (Promega) according to the manufacturer's instructions. Firefly and Renilla luciferase activities were measured using Varioskan Flash (Thermo fisher scientific). Following authentication based on renilla activity, the result was expressed as the fold change between LSD1 inhibition and control.

2.9. Statistical analyses

Welch's t-tests were used for statistical comparison between the two samples.

3. Results

1. LSD1 inhibitor leads *Vimentin* expression in epithelial phenotype OM-1 cells.

Since it was known that chemical LSD1 inhibitors promoted the development of epithelial lineages [6], we initially applied a chemical LSD1 inhibitor TCP to oral SCC cell-line OM-1 cells, which have the ability to form multilayered epithelial structures *in vitro* [11–13]. Surprisingly, the addition of TCP induced EMT of OM-1 cells as visualized by immunocytochemistry with Vimentin (Fig. 1A and B). The wound healing assay further confirmed the LSD1 inhibitor was able to accelerate single-cell migration (Fig. 1C). Therefore we next analyzed the mRNA expression of EMT markers together with the anticipated elevation of epithelial progenitor markers such as *OVOL* and *GRHL* [6] (Fig. 1D). The epithelial regulator *OVOL2*, *GRHL1*, *GRHL2*, and *GRHL3* were up-regulated (Fig. 1D) while functionally opposite EMT-regulator *ZEB1* and EMT-marker *Vimentin* displayed marked induction upon the LSD1 inhibitor treatment in a time-dependent manner (Fig. 1D). *ZEB1* induction was also confirmed by immunocytochemistry (Fig. 1A and B), which demonstrated the coincidence of *Zeb1* induction with Vimentin (Fig. 1A). The cells with assembled Vimentin lost E-cadherin; however, the cells with unassembled Vimentin had E-cadherin (Fig. 1A), indicating the chemical inhibition of LSD1 lead OM-1 cells to undergo both partial EMT and EMT (Fig. 1B). Application of another LSD1 inhibitor, GSK-LSD1 had similar results (Fig. 1 A, 1B, and 1D), confirming chemical LSD1 inhibition-dependent EMT in OM-1 cells.

2. LSD1 inhibitor promotes partial EMT phenotype cells to complete EMT.

An EMT-TF Snail had been reported to physically associate with LSD1 to exhibit transcriptional repression for target genes [7]. As we previously reported that exogenous *Snail*-induced OM-1 cells, referred to as pEMT OM-1^{Snail} cells, gained Snail-dependent partial EMT phenotype [14] with both *CDH1* and *Vimentin* expressions

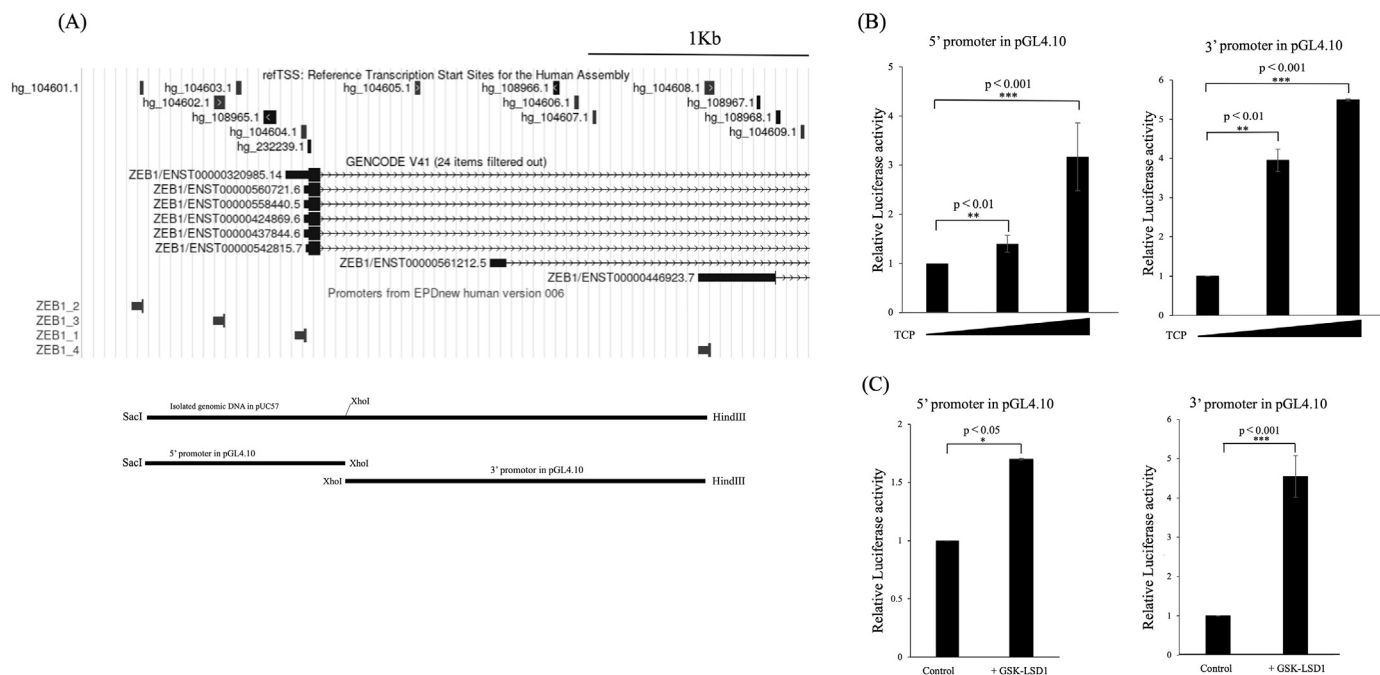


Fig. 3. LSD1 inhibitor-induced transcriptional activation of *ZEB1*.

(A) Schematic representation of the promoter region of *ZEB1*.

The schema was from UCSC Genome Browser on Human (GRCh38/hg38). The regions for luciferase reporter constructs were indicated as 5' promoter and 3' promoter, respectively.

(B) The separated *ZEB1* promoter activities in HEK293 cells with exposure to varying amounts of TCP for 12 h. Transfection efficiency were normalized by Renilla in the dual luciferase assay. The results were from 3 experiments with SD. Statistical analyses were performed between indicated groups.

(C) The separated *ZEB1* promoter activities in HEK293 cells with GSK-LSD1 treatment for 12 h. The results were from 3 experiments with SD. Statistical analysis were performed between indicated groups.

[10,15], we next tested whether the chemical LSD1 inhibition lead pEMT OM-1^{Snail} cells to complete EMT. The pEMT OM-1^{Snail} cells constantly expressed *Vimentin* and *CDH1* but not *ZEB1* (Fig. 2A) with unassembled Vimentin (Fig. 2B). Application of the LSD1 inhibitor lead pEMT OM-1^{Snail} cells to express *ZEB1* with coinciding assembling of fibrous Vimentin (Fig. 2A and B). The pEMT OM-1^{Snail} cells constantly express exogenous *Snail*, *Vimentin*, and the epithelial lineages *CDH1*, and *OVOL2*, while the chemical LSD1 inhibition induced *ZEB1* together with the further upregulations of *Vimentin* and opposite epithelial regulator *OVOL2*, *GRHL1*, *GRHL2*, and *GRHL3* (Fig. 2A). *ZEB1*-knockdown suppressed the induction of *Vimentin* by the LSD1 inhibitor in OM-1 cells (Fig. 2C); however, high and constant expression of Vimentin in pEMT OM-1^{Snail} was not abrogated (Fig. 2C), suggesting the LSD1 inhibitor had the ability to complete EMT via *ZEB1* induction without affecting *Snail*-dependent Vimentin expression.

3. LSD1 inhibitor promotes *ZEB1* promoter activity.

As schematically presented in Fig. 3A, the human *ZEB1* gene had been found to possess several transcription-start-sites (TSSs) with three different exons, two of which possessed alternative initiation codons. To determine the chemical LSD1 inhibition-dependent transcriptional activation of *ZEB1*, we constructed luciferase reporters, which contained different promoter regions (Fig. 3A). Luciferase reporter activities in HEK293 cells were released in response to the LSD1 inhibitor in a dose-dependent manner (Fig. 3B). GSK-LSD1 also released these promoter activities (Fig. 3C), suggesting LSD1 is associated with the separate chromatin regions

for suppression of *ZEB1*.

4. LSD1 accumulates at the *ZEB1* regulatory chromatin region to modify the histone mark.

Since chemical LSD1 inhibition caused *ZEB1* activation at two separate promoters, we assumed LSD1 accumulated to those chromatin regions to suppress *ZEB1*. As potential LSD1 accumulation around the TSSs of *ZEB1* were verified using the ChIP-atlas database [16] (<https://chip-atlas.org/>) (Fig. 3A) and the Gene Expression Omnibus database [17] (GEO, <http://www.ncbi.nlm.nih.gov/geo/>), we tested whether LSD1 co-immunoprecipitated with the specific sequences using ChIP-qPCR assay (Fig. 4A). The accumulation of LSD1 at the specific chromatin regions (Fig. 4A) was lost by the chemical LSD1 inhibition (Fig. 4B) in both OM-1 and pEMT OM-1^{Snail}, indicating LSD1-dependent suppression of *ZEB1* in these cells. Since LSD1 has been known to exhibit specific histone H3 demethylase activity at di-methylated lysine 4 (H3K4me2), we further performed ChIP-qPCR using an anti-H3K4me2 antibody to test the possible histone mark alteration around the LSD1-accumulated *ZEB1* chromatin regions (Fig. 4A) by the chemical inhibition of LSD1 (Fig. 4B). The chemical LSD1 inhibition caused accumulations of H3K4me2 around the separated promoter regions (Fig. 4A), which exhibited LSD1 inhibition-dependent transcriptional activation (Fig. 3B), in both OM-1 and pEMT OM-1^{Snail} (Fig. 4B).

Taken all together, LSD1 suppressed *ZEB1* transcription and its chemical inhibitor released *ZEB1*-dependent EMT program of oral SCC cell OM-1.

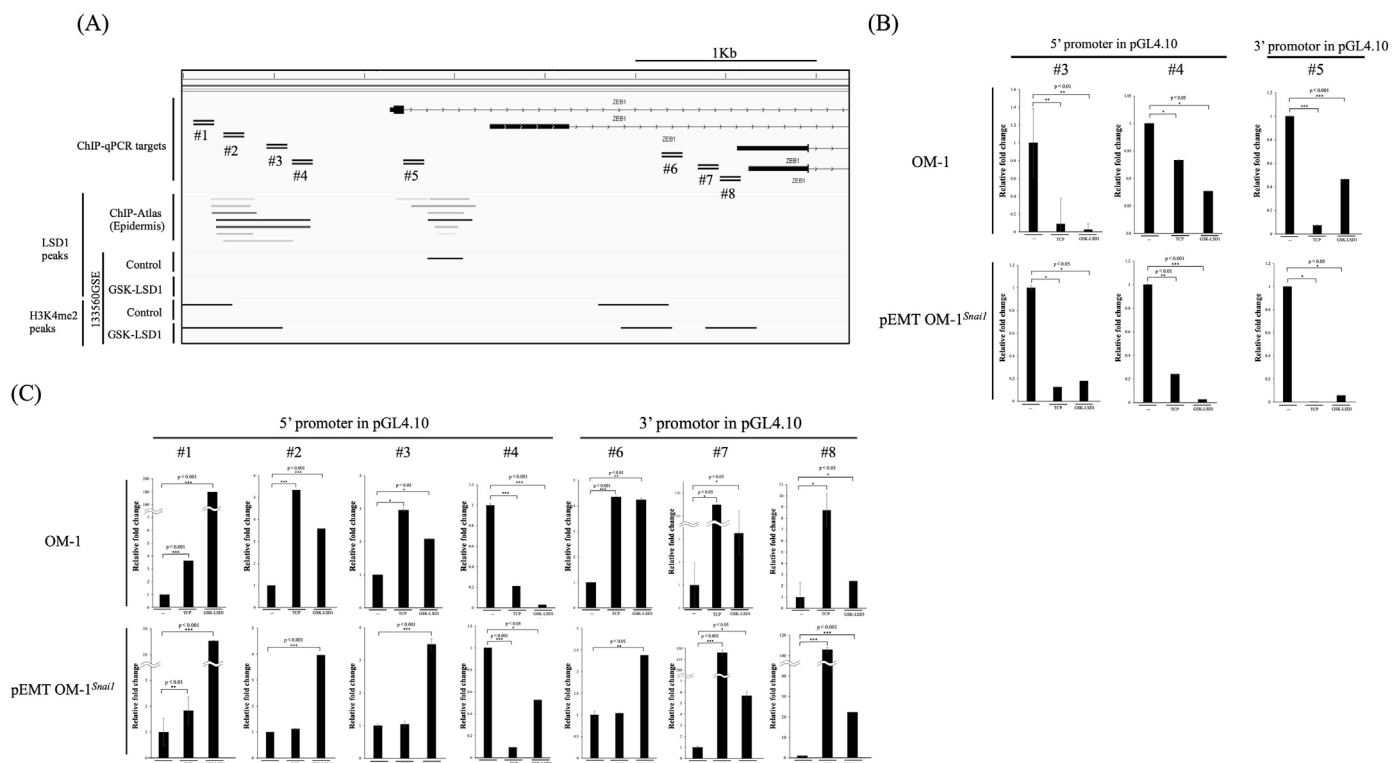


Fig. 4. LSD1 inhibitor altered accumulation of LSD1 and its substrate histone methylation mark around *ZEB1* promoter chromatin regions. (A) Schema of curated LSD1 and H3K4me2 peaks around *ZEB1* promoter regions from public ChIP-seq database ChIP-Atlas (<https://chip-atlas.org/>) [16]. The peaks of GSK-LSD1-treated and its control normal human epidermal keratinocytes ChIP-seq results were from GSE133560 [6]. The target chromatin regions analyzed by ChIP-qPCR in this work were also indicated with names (#1-#8). The diagram was based on the Integrative Genomics Viewer [22] (B) The relative changes of LSD1 enrichment in response to indicated LSD1 inhibitors at the indicated chromatin regions of *ZEB1* promoters in OM-1 cells and pEMT OM-1^{Snail} cells. The results were from 3 experiments with SD. Statistical analysis were performed between indicated groups. (C) The relative changes of H3K4me2 enrichment in response to indicated LSD1 inhibitors at the indicated chromatin regions of *ZEB1* promoters in OM-1 cell and pEMT OM-1^{Snail} cell. The results were from 3 experiments with SD. Statistical analysis were performed between indicated groups.

4. Discussion

In this work, we found LSD1 association at different chromatin regions of *ZEB1* located upstream of alternative TSSs, where the promoter activities were released by the chemical LSD1 inhibition. The chromatin landscape which lost LSD1 loading by chemical LSD1 inhibition had been reported [6], and we analyzed the uploaded GSE133560 ChIP-seq data [6] to determine possible H3K4me2 accumulations around LSD1-lost chromatin region of *ZEB1* TSSs as schematically presented in Fig. 4A. The histone mark H3K4me2 around *ZEB1* promoters was consistently increased by chemical inhibition of LSD1, leading to active chromatin for *ZEB1*. Our previous works demonstrated oral SCC OM-1 cells created both epithelial progenitor and CSC populations [18,19]. The cell plasticity of non-CSC to CSC had been reported, and non-CSC population exhibited poised chromatin around the second TSS of *ZEB1* [20]. The microenvironmental cue provides activation of the poised chromatin to lead ZEB1-dependent conversion of non-CSC to CSC of which gene profile was shared by the EMT [20]. Our results in this work suggested only chemical inhibition of LSD1 was able to promote ZEB1-dependent EMT program, which might associated with non-CSC to CSC conversion in oral SCC cells, adverting to cancer therapeutics.

LSD1 had been known to associate with another EMT-TF snail, and our previous work demonstrated Snail-LSD1 interaction on chromatin in OM-1 cells associated with the conversion of partial EMT to EMT [15]. We previously reported that exogenous *Snail* expression in OM-1 led to partial EMT, which had *CDH1*, *OVOL2*, and *Vimentin* but not *Slug* and *ZEB1*. We anticipated LSD1 inhibition might revert partial EMT to epithelial phenotype through abrogated LSD1-dependent Snail functions; however, *ZEB1* induction by the chemical inhibition of LSD1 in pEMT OM-1^{Snail} promotes to complete EMT program. Although epidermal differentiation by LSD1 inhibitor had been reported and our results in OM-1 and pEMT OM-1^{Snail} also demonstrated upregulation of *CDH1* as well as epithelial regulators *OVOL* and *GRHL* by the chemical inhibition of LSD1, which is believed to be favorable to cancer therapeutics, we should care the adverse effect via induction of *ZEB1*.

The limitation of this work was, we performed only bulk analysis for RNA expressions. Epithelial-, partial EMT-, and EMT-phenotype coexist under the chemical inhibition of LSD1. Single-cell analysis strategy may reveal a fate-determining mechanism under LSD1 inhibition. Since LSD1-containing H3K4me2 demethylation complex on 5'promoter of *ZEB1* had been proposed in a previous report [21], we also need to determine the LSD1-containing complex with the pioneer factor to bind *ZEB1* promoter/enhancer element for *ZEB1* suppression.

Author contributions and fundings

NY performed all experimental work, data analysis, and writing. SO also performed experimental works and data analysis. KT contributed to designing the experiments, analyzing data, and writing the manuscript. RY, SO, KM, TN, and TA provided materials and contributed to the manuscript's review and editing. This work was funded by the Japan Society for the Promotion of Science grants-in-aid (KAKENHI) as follows: JP22K10171 (KT), JP22K17158 (RY), JP20K10139 (SO), JP22K10119(KM), JP21K10094 (TN), and JP22K10145 (TA).

Declaration of competing interest

The authors have no potential conflicts of interest to declare.

Acknowledgements

We would like to thank Enago (www.enago.jp) for the English language editing.

Appendix A. Supplementary data

Supplementary data to this article can be found online at <https://doi.org/10.1016/j.bbrc.2023.01.062>.

References

- [1] H. Peinado, D. Olmeda, A. Cano, Snail, ZEB and bHLH factors in tumour progression: an alliance against the epithelial phenotype? *Nat. Rev. Cancer* 7 (2007) 415–428, <https://doi.org/10.1038/NRC2131>.
- [2] J. Wang, K. Scully, X. Zhu, L. Cai, J. Zhang, G.G. Prefontaine, A. Krones, K.A. Ohgi, P. Zhu, I. Garcia-Bassets, F. Liu, H. Taylor, J. Lozach, F.L. Jayes, K.S. Korach, C.K. Glass, X.D. Fu, M.G. Rosenfeld, Opposing LSD1 complexes function in developmental gene activation and repression programmes, *Nature* 446 (2007) 882–887, <https://doi.org/10.1038/nature05671>, 2006 4467138.
- [3] N.K. Vinckier, N.A. Patel, R.J. Geusz, A. Wang, J. Wang, I. Matta, A.R. Harrington, M. Wortham, N. Wetton, J. Wang, U.S. Jhala, M.G. Rosenfeld, C.W. Benner, H.P. Shih, M. Sander, LSD1-mediated enhancer silencing attenuates retinoic acid signalling during pancreatic endocrine cell development, *Nat. Commun.* 11 (2020), <https://doi.org/10.1038/S41467-020-16017-X>.
- [4] Y. Fang, G. Liao, B. Yu, LSD1/KDM1A inhibitors in clinical trials: advances and prospects, *J. Hematol. Oncol.* 12 (2019), <https://doi.org/10.1186/S13045-019-0811-9>.
- [5] S. Zhang, M. Liu, Y. Yao, B. Yu, H. Liu, Targeting LSD1 for acute myeloid leukemia (AML) treatment, *Pharmacol. Res.* 164 (2021), <https://doi.org/10.1016/j.phrs.2020.105335>.
- [6] S. Egoif, Y. Aubert, M. Doepner, A. Anderson, A. Maldonado-Lopez, G. Pacella, J. Lee, E.K. Ko, J. Zou, Y. Lan, C.L. Simpson, T. Ridky, B.C. Capell, LSD1 inhibition promotes epithelial differentiation through derepression of fate-determining transcription factors, *Cell Rep.* 28 (2019) 1981–1992.e7, <https://doi.org/10.1016/j.celrep.2019.07.058>.
- [7] T. Lin, A. Ponn, X. Hu, B.K. Law, J. Lu, Requirement of the histone demethylase LSD1 in Snai1-mediated transcriptional repression during epithelial-mesenchymal transition, *Oncogene* 29 (2010) 4896–4904, <https://doi.org/10.1038/ncr.2010.234>.
- [8] G. Ferrari-Amorotti, V. Fragiasso, R. Esteki, Z. Prudente, A.R. Soliera, S. Cattelani, G. Manzotti, G. Grisendi, M. Dominici, M. Pieraccioli, G. Raschella, C. Chiodoni, M.P. Colombo, B. Calabretta, Inhibiting interactions of lysine demethylase LSD1 with snail/slugs blocks cancer cell invasion, *Cancer Res.* 73 (2013) 235–245, <https://doi.org/10.1158/0008-5472.CAN-12-1739>.
- [9] M. Wang, X. Liu, J. Guo, X. Weng, G. Jiang, Z. Wang, L. He, Inhibition of LSD1 by Pargyline inhibited process of EMT and delayed progression of prostate cancer in vivo, *Biochem. Biophys. Res. Commun.* 467 (2015) 310–315, <https://doi.org/10.1016/j.bbrc.2015.09.164>.
- [10] G. Okui, K. Tobiume, A. Rizqiawan, K. Yamamoto, H. Shigeishi, S. Ono, K. Higashikawa, N. Kamata, AKT primes snail-induced EMT concomitantly with the collective migration of squamous cell carcinoma cells, *J. Cell. Biochem.* 114 (2013) 2039–2049, <https://doi.org/10.1002/jcb.24545>.
- [11] K. Higashikawa, S. Yoneda, K. Tobiume, M. Saitoh, M. Taki, Y. Mitani, H. Shigeishi, S. Ono, N. Kamata, ΔNp63α-dependent expression of Id-3 distinctively suppresses the invasiveness of human squamous cell carcinoma, *Int. J. Cancer* 124 (2009) 2837–2844, <https://doi.org/10.1002/ijc.24280>.
- [12] A. Rizqiawan, K. Tobiume, G. Okui, K. Yamamoto, H. Shigeishi, S. Ono, H. Shimasue, M. Takechi, K. Higashikawa, N. Kamata, Autocrine galectin-1 promotes collective cell migration of squamous cell carcinoma cells through up-regulation of distinct integrins, *Biochem. Biophys. Res. Commun.* 441 (2013) 904–910, <https://doi.org/10.1016/j.bbrc.2013.10.152>.
- [13] F. Tanaka, A. Rizqiawan, K. Higashikawa, K. Tobiume, G. Okui, H. Shigeishi, S. Ono, H. Shimasue, N. Kamata, Snail promotes Cyr61 secretion to prime collective cell migration and form invasive tumor nests in squamous cell carcinoma, *Cancer Lett.* 329 (2013) 243–252, <https://doi.org/10.1016/j.canlet.2012.11.023>.
- [14] I. Pastushenko, C. Blanpain, EMT transition states during tumor progression and metastasis, *Trends Cell Biol.* 29 (2019) 212–226, <https://doi.org/10.1016/j.tcb.2018.12.001>.
- [15] S. Okuda, N. Yamakado, K. Higashikawa, R. Uetsuki, F. Ishida, A. Rizqiawan, S. Ono, K. Mizuta, N. Kamata, K. Tobiume, Dexamethasone resets stable association of nuclear Snail with LSD1 concomitant with transition from EMT to partial EMT, *Biochem. Biophys. Reports.* 30 (2022), <https://doi.org/10.1016/j.bbrep.2022.101277>.
- [16] S. Oki, T. Ohta, G. Shioi, H. Hatanaka, O. Ogasawara, Y. Okuda, H. Kawaji, R. Nakaki, J. Sese, C. Meno, ChIP-Atlas: a data-mining suite powered by full integration of public ChIP-seq data, *EMBO Rep.* 19 (2018), e46255, <https://doi.org/10.15252/EMBR.201846255>.
- [17] T. Barrett, S.E. Wilhite, P. Ledoux, C. Evangelista, I.F. Kim, M. Tomashevsky, K.A. Marshall, K.H. Phillippy, P.M. Sherman, M. Holko, A. Yefanov, H. Lee,

- N. Zhang, C.L. Robertson, N. Serova, S. Davis, A. Soboleva, NCBI GEO: archive for functional genomics data sets—update, *Nucleic Acids Res.* 41 (2013) D991, <https://doi.org/10.1093/NAR/GKS1193>. –D995.
- [18] R. Uetsuki, K. Higashikawa, S. Okuda, N. Yamakado, F. Ishida, A. Rizqiawan, S. Ono, M. Takechi, K. Mizuta, H. Shigeishi, N. Kamata, K. Tobiume, The squamous cell carcinoma cell line OM-1 retains both p75-dependent stratified epithelial progenitor potential and cancer stem cell properties, *Biochem. Biophys. Reports.* 26 (2021), <https://doi.org/10.1016/j.bbrep.2021.101003>.
- [19] S. Seino, H. Shigeishi, M. Hashikata, K. Higashikawa, K. Tobiume, R. Uetsuki, Y. Ishida, K. Sasaki, T. Naruse, M.Z. Rahman, S. Ono, H. Simasue, K. Ohta, M. Sugiyama, M. Takechi, CD44^{high}/ALDH1^{high} head and neck squamous cell carcinoma cells exhibit mesenchymal characteristics and GSK3 β -dependent cancer stem cell properties, *J. Oral Pathol. Med.* 45 (2016) 180–188, <https://doi.org/10.1111/jop.12348>.
- [20] C.L. Chaffer, N.D. Marjanovic, T. Lee, G. Bell, C.G. Kleer, F. Reinhardt, A.C. D'Alessio, R.A. Young, R.A. Weinberg, Poised chromatin at the ZEB1 promoter enables breast cancer cell plasticity and enhances tumorigenicity, *Cell* 154 (2013) 61, <https://doi.org/10.1016/j.cell.2013.06.005>.
- [21] H. Choi, J. Park, M. Park, H. Won, H. Joo, C.H. Lee, J. Lee, G. Kong, UTX inhibits EMT-induced breast CSC properties by epigenetic repression of EMT genes in cooperation with LSD 1 and HDAC 1, *EMBO Rep.* 16 (2015) 1288–1298, <https://doi.org/10.15252/EMBR.201540244>.
- [22] J.T. Robinson, H. Thorvaldsdóttir, W. Winckler, M. Guttman, E.S. Lander, G. Getz, J.P. Mesirov, Integrative genomics viewer, *Nat. Biotechnol.* 29 (2011) 24–26, <https://doi.org/10.1038/nbt.1754>, 2011 291.